Measurement of dielectrons in pp, p–Pb and Pb–Pb collisions with ALICE at the LHC

Alberto Calivà on behalf of the ALICE Collaboration
NIKHEF Institite for subatomic physics and Utrecht University, Utrecht, NL
E-mail: alberto.caliva@cern.ch

Abstract.
Dielectrons are penetrating probes which carry unaffected information on the hot and dense medium created in ultra-relativistic heavy-ion collisions. The low-mass region of the dielectron spectrum ($m_{\pi^0} < m_{\rm ee} < m_\rho$) is sensitive to virtual photon production and in-medium modifications of low-mass vector meson spectral functions. These modifications are connected to the restoration of chiral symmetry, which is expected at high temperature. Dielectrons are also sensitive to heavy-flavor production.

In these proceedings, we present the preliminary results of dielectron measurements in pp collisions at $\sqrt{s} = 7$ TeV, in p–Pb collisions at $\sqrt{s_{\rm NN}} = 5.02$ TeV and in central (0-10%) Pb–Pb collisions at $\sqrt{s_{\rm NN}} = 2.76$ TeV with the ALICE experiment at the LHC. The expected scenario and perspectives for the dielectron measurement after the ALICE upgrade are also discussed.

1. Introduction

Photons and dileptons are emitted continuously during the expansion of the hot and dense medium created in ultra-relativistic heavy-ion collisions [1]. The temperature of the system can be extracted from the direct photon $p_{\rm T}$-spectrum and from the dielectron invariant-mass distribution, with the advantage that in the latter the measurement is not affected by the Doppler shift caused by the rapid expansion of the emitting source.

Different regions of the dielectron spectrum are particularly sensitive to different stages of the collision. The low-mass region ($m_{\rm ee} < m_\rho$) is interesting for studying the production of virtual direct photons and the modifications of the ρ-meson spectral properties in the hot hadron gas phase. These are connected to the chiral symmetry restoration, which is expected at high temperatures [2]. Dielectrons are also sensitive to heavy-flavor production.

2. Data analysis strategy

The ALICE experimental apparatus is described in detail in [3]. The main detectors used in the data analysis are the Inner Tracking System (ITS) (for vertexing, tracking and particle identification), the Time Projection Chamber (TPC) (for tracking and particle identification) and the Time-Of-Flight (TOF) detector (for particle identification). In Pb–Pb collisions the centrality selection has been done using the measured multiplicity in the V0 detector.

Track selection criteria have been optimized to ensure a good overall quality of the tracks and to reject secondary tracks, particularly those from photon conversion in the material. Electron identification has been based on the measurement of the average energy loss per unit path length

in the TPC and ITS and on the time-of-flight measurement in the TOF detector.

The background has been estimated using the like-sign spectrum, corrected for acceptance effects using the event-mixing. The efficiency calculation has been based on MC simulations including a realistic description of the detector effects.

3. Results in pp and p–Pb collisions

The dielectron invariant-mass spectra measured in pp collisions at $\sqrt{s} = 7$ TeV and in p–Pb collisions at $\sqrt{s_{\rm NN}} = 5.02$ TeV have been compared to the expected contributions from hadronic sources, called *hadronic cocktail*.

The cocktail has been generated using the parametrizations of the $p_{\rm T}$-differential cross sections of π^0, η, ϕ and J/ψ measured by ALICE [4, 5, 6] in pp collisions, and those of charged pions for p–Pb collisions [7]. The remaining contributions from light-flavored mesons have been obtained using $m_{\rm T}$ scaling. The charm contribution in pp collisions has been obtained from PYTHIA 6, scaled to $\sigma_{\rm c\bar{c}}$ measured by ALICE at $\sqrt{s} = 7$ TeV [8]. In p–Pb collisions, the charm and beauty contributions have been obtained using the interpolated values of $\sigma_{\rm c\bar{c}}$ and $\sigma_{\rm b\bar{b}}$ at $\sqrt{s_{\rm NN}} = 5.02$ TeV and scaling the spectra by the average number of binary collisions $\langle N_{\rm coll}\rangle$.

In both collision systems no enhanced dielectron yield is expected in the low-mass region. The measured invariant-mass spectra are in agreement with the cocktail within the statistical and systematic uncertainties (Fig. 1).

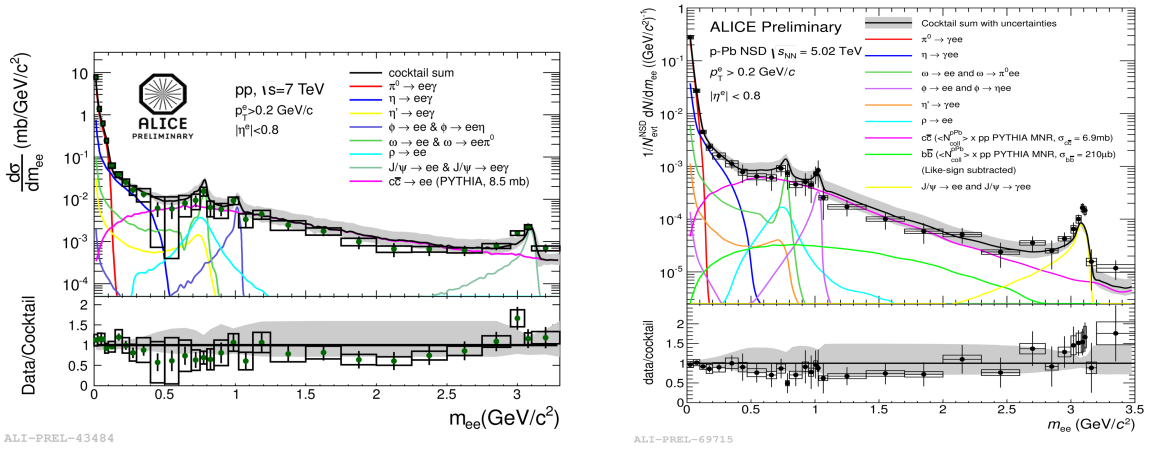

Figure 1. Dielectron invariant mass spectrum measured in pp collisions at $\sqrt{s} = 7$ TeV (left) and in p–Pb collisions at $\sqrt{s_{\rm NN}} = 5.02$ TeV (right) compared to the hadronic cocktail.

The virtual photon contribution has been extracted in pp collisions from the two-component fit in the kinematic range $p_{\rm T}^{\rm ee} \gg m_{\rm ee}$: $f(m_{\rm ee}) = r \cdot f_{dir}(m_{\rm ee}) + (1\text{-}r) \cdot f_c(m_{\rm ee})$, where f_{dir} is the mass distribution of virtual photons, given by the Kroll-Wada formula [10], and f_c is the cocktail shape. The fraction r of virtual direct photons extracted from the fit is consistent with the measurement of real direct photons using the photon conversion method (PCM) (Fig. 2) [11]. The virtual direct photon invariant cross section measured in pp collisions is consistent with NLO pQCD calculations [13].

4. Results in Pb–Pb collisions

The first measurement of the dielectron invariant-mass spectrum in central Pb–Pb collisions at $\sqrt{s_{\rm NN}} = 2.76$ TeV is shown in Fig. 3 in comparison with the hadronic cocktail.

The $p_{\rm T}$-differential cross section of π^0 [12] has been used as input parametrization, while $m_{\rm T}$ scaling was applied to obtain the remaining contributions of light-flavored mesons. The

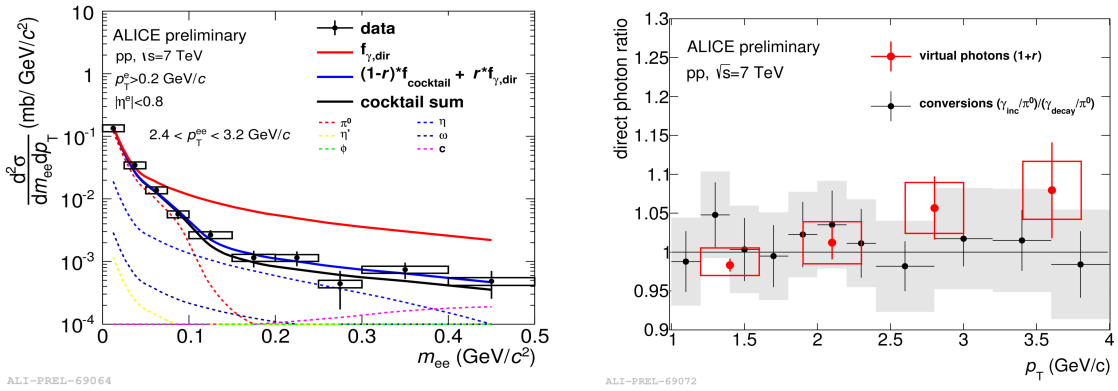

Figure 2. (Left) Example of the two-component fit to the dielectron spectrum in the low-mass region. (Right) Real direct photon ratio ($\gamma_{incl}/\gamma_{decay}$) measured in pp collisions at $\sqrt{s}$ = 7 TeV with the Photon Conversion Method (black) [11] compared to virtual direct photon ratio (1+r) (red) from the dielectron measurement. The real photon measurement is consistent with zero direct photon yield within uncertainties, while the virtual photon measurement indicates a non-zero yield for $p_T > 2.5$ GeV/c.

contributions from charm and beauty decays have been obtained from PYTHIA 6 for pp collisions at $\sqrt{s_{NN}}$ = 2.76 TeV (using $\sigma_{c\bar{c}}$ = 4.8 mb [8] and $\sigma_{b\bar{b}}$ = 130 μb [9]), and scaled by the average number of binary collisions. Energy losses of charm quarks in the medium are ignored.

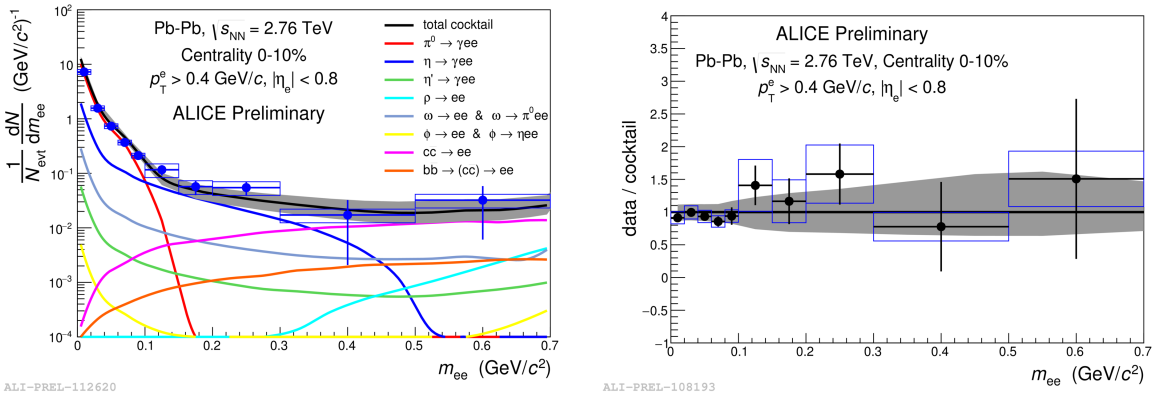

Figure 3. Dielectron invariant-mass spectrum measured in Pb–Pb collisions at $\sqrt{s_{NN}}$ = 2.76 TeV compared to the hadronic cocktail (left) and data-to-cocktail ratio (right).

While an enhanced dielectron production is expected in Pb–Pb collisions, originating from the QGP thermal radiation and the in-medium modification of the ρ-meson, the data-to-cocktail ratio is consistent with unity within the uncertainties.

An upper limit on the virtual photon production has been estimated at 90% C.L. (Fig. 4), from the analysis of the mass region $100 < m_{ee} < 300$ MeV/c^2, which is consistent with the real photon measurement by ALICE [14] and previous dielectron measurements from PHENIX and STAR at $\sqrt{s_{NN}}$ = 200 GeV [15, 16].

5. Perspectives after the ALICE upgrade

The perspectives for the dielectron measurement after the ALICE upgrade for Run 3 at the LHC have been studied. The new ITS [17], with improved resolution in the determination of secondary vertices and reduced material budget, will allow a better suppression of the main background

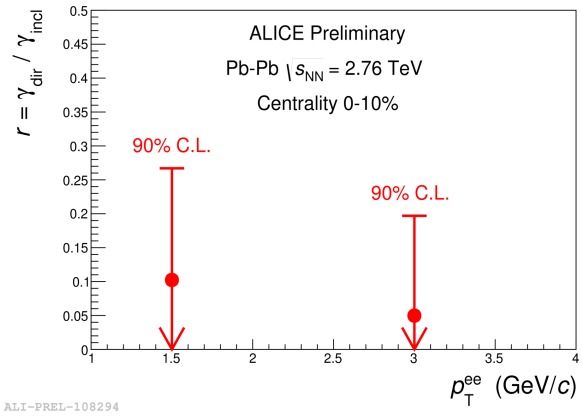

Figure 4. Upper limit at 90 % C.L. on virtual photon production in Pb–Pb collisions at $\sqrt{s_{\rm NN}} = 2.76$ TeV.

contributions (Dalitz and charm decays, photon conversions), and the continuous TPC readout will increase the event rate by a factor ~ 100 [18]. This will allow a precise measurement of the QGP temperature, from a fit to the intermediate mass region, and a detailed study of the in-medium modifications of the ρ-meson [19].

6. Conclusions

Dielectron invariant mass spectra have been measured in the three different collision systems at different energies. In pp collisions the measured contribution of virtual direct photons is consistent with the PCM measurement of real photons, and the direct photon invariant cross section is consistent with NLO pQCD calculations. In p–Pb collisions the dielectron spectrum is in agreement with the hadronic cocktail within the uncertainties. In Pb–Pb collisions, the extracted upper limit at 90% C.L. on virtual photon production is consistent with the real photon measurement from ALICE and previous dielectron measurements from PHENIX and STAR at RHIC. Regarding the expected scenario after the upgrade, the simulations indicate an improved significance of the temperature measurement and an enhanced sensitivity to in-medium effects of the ρ-meson with upgraded detectors and enhanced statistics in Run 3 at the LHC.

References

[1] J-e. Alam, S. Raha, and B. Sinha, Physics Reports, 273, pp. 243–362 (1996).
[2] R. Rapp and J. Wambach, Advances in Nuclear Physics, 25, pp. 1–205 (2000).
[3] K. Aamodt et al. (The ALICE Collaboration) JINST, 3, S08002 (2008).
[4] K. Koch (The ALICE Collaboration), Nucl. Phys. A, 855, pp. 281–284 (2011).
[5] B. Abelev et al. (The ALICE Collaboration), Eur. Phys. J. C, 72, p. 2183 (2012).
[6] K. Aamodt et al. (The ALICE Collaboration), Phys. Lett. B, 704, pp. 442–455 (2011).
[7] B. Abelev et al. (The ALICE Collaboration), Phys. Rev. Lett., 110, 082302 (2013).
[8] B. Abelev et al. (The ALICE Collaboration), J. High Energ. Phys. (2012).
[9] B. Abelev et al. (The ALICE Collaboration), Phys. Lett. B, 738, p. 97 (2014).
[10] N. Kroll, W. Wada, Phys. Rev., 98, p. 1355 (1955).
[11] J. Adam et al. (The ALICE Collaboration), Phys. Lett. B, 754, pp. 235–248 (2016).
[12] B. Abelev et al. (The ALICE Collaboration), Eur. Phys. J. C, 74, 10, p. 3108 (2014).
[13] Markus K. Kohler (The ALICE Collaboration), Nuclear Physics A 00 14 (2014).
[14] J. Adam et al. (The ALICE Collaboration), Phys. Lett. B, 754, pp. 235–248 (2016).
[15] A. Adare et al. (The PHENIX Collaboration), Phys. Rev. C, 93, 014904 (2016).
[16] L. Adamczyk et al. (The STAR Collaboration), Phys. Rev. Lett., 113, 022301 (2014).
[17] CERN-LHCC-2013-024, ALICE-TDR-017.
[18] CERN-LHCC-2013-020, ALICE-TDR-016.
[19] B. Abelev et al. (The ALICE Collaboration), J. Phys. G, 41, 087002 (2014).